The kalimantacin polyketide antibiotics inhibit fatty acid biosynthesis in *Staphylococcus aureus* by targeting the enoyl-acyl carrier protein binding site of FabI

Christopher D Fage[†], Thomas Lathouwers[†], Michiel Vanmeert, Ling-Jie Gao, Kristof Vrancken, Eveline-Marie Lammens, Angus NM Weir, Ruben Degroote, Harry Cuppens, Simone Kosol, Thomas J Simpson, Matthew P Crump, Christine L Willis, Piet Herdewijn, Eveline Lescrinier, Rob Lavigne, Jozef Anné and Joleen Masschelein*

Abstract: The enoyl-acyl carrier protein reductase enzyme FabI is essential for fatty acid biosynthesis in *Staphylococcus aureus* and represents a promising target for the development of novel, urgently needed anti-staphylococcal agents. Here, we elucidate the mode of action of the kalimantacin antibiotics, a novel class of FabI inhibitors with clinically-relevant activity against multidrug-resistant *S. aureus*. By combining X-ray crystallography with molecular dynamics simulations, *in vitro* kinetic studies and chemical derivatization experiments, we characterize the interaction between the antibiotics and their target, and we demonstrate that the kalimantacins bind in a unique conformation that differs significantly from the binding mode of other known FabI inhibitors. We also investigate mechanisms of acquired resistance in *S. aureus* and identify key residues in FabI that stabilize the binding of the antibiotics. Our findings provide intriguing insights into the mode of action of a novel class of FabI inhibitors that will inspire future anti-staphylococcal drug development.

Staphylococcus aureus is a notorious human pathogen responsible for a wide range of hospital- and community-acquired infections with life-threatening complications, such as septicemia, pneumonia, endocarditis and meningitis.[1] The continuing global evolution and spread of multidrug-resistant strains of *S. aureus,* such as methicillin-resistant *S. aureus* (MRSA), remains one of the major concerns for healthcare institutions worldwide, and novel anti-staphylococcal agents are therefore urgently needed.[2] An attractive and relatively underexploited target for antibacterial drug development in *S. aureus* is the fatty acid biosynthetic pathway (FAS-II).[3] Fatty acids are essential components of cell membranes and cannot be scavenged from the human host.[4] Furthermore, the bacterial FAS-II pathway differs significantly from the mammalian FAS-I system, which utilizes a multi-functional, multi-domain enzyme rather than discrete enzymes to catalyze each step in the fatty acid chain elongation cycle.[5] Inhibitors of bacterial fatty acid biosynthesis are therefore considered to be selective and safe for use in humans. The most frequently targeted enzyme in the FAS-II pathway is the NADPH-dependent enoyl-acyl carrier protein (ACP) reductase (ENR) enzyme FabI, which catalyses the final and rate-limiting step of the elongation cycle.[6] FabI is essential to cell viability and is a validated drug target in *S. aureus*.[4,7] Several bacterial species have been reported to utilize alternative ENR isozymes, such as FabL in *Bacillus subtilis*, FabK in *Streptococcus pneumoniae* and FabV in *Vibrio cholera*.[8] Due to differences in secondary structure and amino acid composition, these isozymes are generally less sensitive to FabI inhibitors.[9] However, FabI is the only ENR isozyme in *S. aureus* and is therefore attracting considerable interest as a target for the development of narrow-spectrum antibiotics to treat MRSA infections.

Kalimantacin A or batumin (KLA, **1**, Figure 1A) is a polyketide antibiotic produced by *Pseudomonas* and *Alcaligenes* spp. that displays selective and clinically-relevant activity against staphylococci, including MRSA.[10-13] It is four- to eight-fold more potent than its *E*,*E*-diene isomer kalimantacin B (KLB, **2**, Figure 1A), isolated from *Alcaligenes* sp. YL-02632S.[12] The kalimantacin antibiotics are assembled by a hybrid polyketide synthase-nonribosomal peptide synthetase (PKS-NRPS) assembly line that exerts remarkable control over the incorporation of different β-branching modifications.[10,14] As linear unsaturated acids and polyenes, the kalimantacins have no analogues among currently used antibiotics in medical practice. Preliminary clinical trials with kalimantacin A, administered as a 0.1% ointment, have indicated that it is highly effective in the treatment and control of nasal *S. aureus* infections.[15] In addition, it has been shown to efficiently disrupt and prevent the formation of *S. aureus* biofilms.[16] Despite its promising biological activity, no further clinical development has been pursued due to a lack of knowledge regarding its precise mechanism of action. Kalimantacin A has been proposed to inhibit FabI in *S. aureus* (saFabI) based on radiolabelled precursor incorporation studies as well as the presence of a FabV-like resistant isoform in the kalimantacin biosynthetic operon in *P. fluorescens*.[17] However, no biochemical or structural data on its mode of action have been reported to date.

To elucidate the molecular basis for the action of kalimantacin A, we pursued a crystal structure of saFabI in complex with the antibiotic and the redox cofactor NADPH. FabI was overproduced in *E. coli* BL21 (DE3) as an N-terminal hexahistidine (His_6) fusion protein and purified to homogeneity

[*] Dr. Christopher D. Fage, Dr. Simone Kosol and Dr. Joleen Masschelein
Department of Chemistry, University of Warwick, CV4 7AL Coventry, United Kingdom

Thomas Lathouwers, Eveline-Marie Lammens, Ruben Degroote and Prof. Rob Lavigne
Laboratory of Gene Technology, KU Leuven, Kasteelpark Arenberg 21, PO Box 2462, 3001 Heverlee, Belgium

Michiel Vanmeert, Dr. Ling-Jie Gao, Prof. Piet Herdewijn, Prof. Eveline Lescrinier and Dr. Joleen Masschelein
Laboratory for Medicinal Chemistry, Rega Institute for Medical Research, Herestraat 49, PO Box 1041, 3000 Leuven, Belgium
email: joleen.masschelein@kuleuven.be

Dr. Kristof Vrancken and Prof. Jozef Anné
Laboratory of Molecular Bacteriology, Rega Institute for Medical Research, Herestraat 49, PO Box 1037, 3000 Leuven, Belgium

Angus N. M. Weir, Prof. Thomas J. Simpson, Prof. Matthew P. Crump and Prof. Christine L. Willis
School of Chemistry, Cantock's Close, University of Bristol, BS8 1TS Bristol, United Kingdom

Prof. Harry Cuppens
Department of Human Genetics, KU Leuven, Herestraat 49, 3000 Leuven, Belgium

[†] These authors contributed equally to this work

Supporting information for this article is given via a link at the end of the document.

by nickel affinity chromatography. UHPLC-ESI-Q-TOF-MS analysis confirmed that the purified protein had the expected molecular weight (Supplementary Figure 1). Following removal of the His_6 tag, saFabI was screened for crystals in a solution containing kalimantacin A and NADPH. A single crystal of a ternary complex diffracted to ~2.45 Å. Once reflections were phased via molecular replacement by searching for two saFabI tetramers (PDB ID 4ALI)[18] in a $P2_12_12_1$ unit cell (Supplementary Table 1), electron density was clearly visible for both the coenzyme and inhibitor (Supplementary Figure 2).

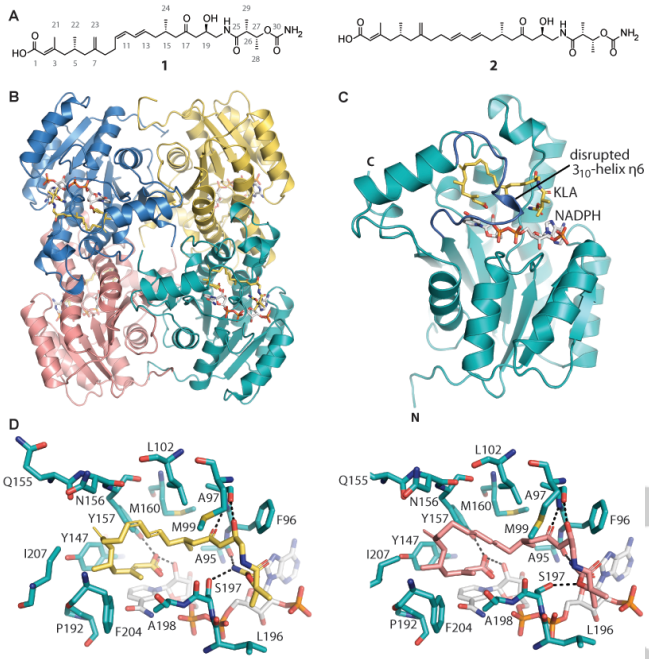

Figure 1. The polyketide antibiotics kalimantacin A and B bind in the hydrophobic substrate channel of FabI from *S. aureus*. (**A**) Structure of kalimantacin A (**1**) and B (**2**). Overall view of a (**B**) tetramer and (**C**) monomer of saFabI bound to kalimantacin A and NADPH. Color code: FabI chains A-D (teal, gold, blue and salmon, respectively), kalimantacin A (KLA, gold carbons) and NADPH (white carbons). SBL-1, which contains 3_{10}-helix η6, is colored blue in panel C. (**D**) Magnified views of the saFabI active site, with kalimantacin A- (left) and B- (right) binding residues labeled. For clarity, V201 is hidden from the foreground. Colored as above, with kalimantacin B (KLB) carbons in salmon.

With NADPH and kalimantacin A bound, FabI assembles into a symmetric homotetramer with nearly ~13,000 $Å^2$ buried between each pair of monomers (Figure 1B),[19] an arrangement that has previously been observed.[18] The overall structure (Figure 1B-D) resembles that of saFabI in complex with $NADP^+$ and triclosan, a well-known inhibitor of FabI that is widely used as a preservative and broad-spectrum biocide (PDB ID 4ALI, Figure 2A and 2C). Kalimantacin A is also located in the active site where the native enoyl-ACP substrate normally binds.[20] However, relative to triclosan, kalimantacin A occupies nearly twice the surface area of the active site (~445 $Å^2$ vs. ~822 $Å^2$, respectively),[19] resulting in disruption of 3_{10}-helix η6 of the substrate binding loop SBL-1 (Gly191-Gly203) (Figure 1C).[20] The antibiotic assumes an inverted ω-shaped conformation, with its center and ends folded inward, resting above NADPH in an elongated binding pocket. The lipophilic alkyl moiety of kalimantacin A is accommodated by the hydrophobic environment of the "left" subpocket, whereas the heteroatom-rich portion of the antibiotic is located in the more hydrophilic "right" subpocket, which opens to solvent (Figure 1D and Supplementary Figure 3). Kalimantacin A binds FabI primarily through van der Waals interactions with L102, Y147, Q155, N156, Y157, M160, P192, A198, V201, F204 and I207 on the "left" side and A95, F96, A97, M99, L196 and S197 on the "right" side. This binding mode differs markedly from those reported for other known classes of FabI inhibitors, such as diphenyl ethers, pyridones, benzimidazoles and naphthyridines, all of which contain one or more ring structures and are invariably located above the nicotinamide ring of the NADP(H)/NAD(H) cofactor in the "left" subpocket (Figure 2).

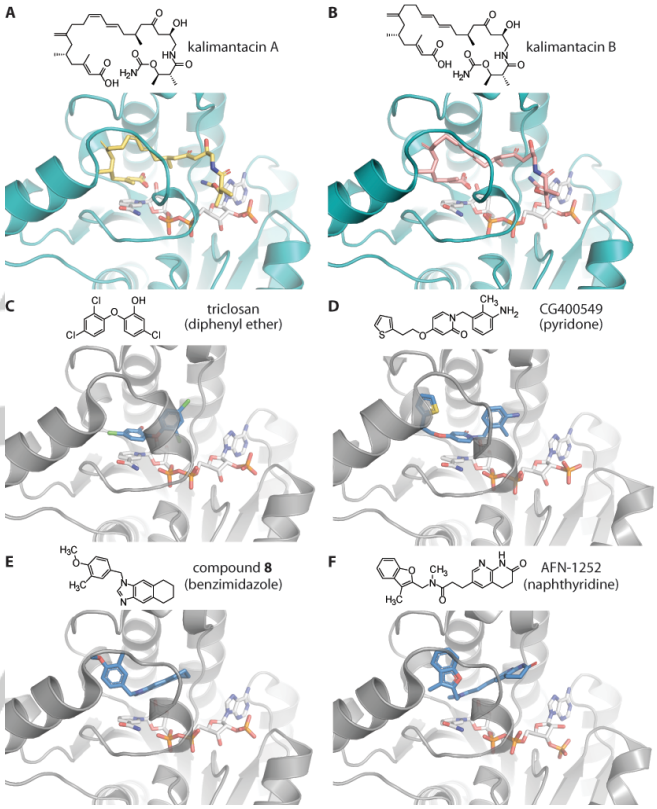

Figure 2. Structures of saFabI monomers bound to representative inhibitors. All panels are shown from the same view after aligning chain A of the relevant structure with that of FabI/NADPH/kalimantacin A (see Cα r.m.s.d. values below). Structure of saFabI bound to (**A**) NADPH/kalimantacin A (PDB ID 6TBB), (**B**) NADPH/kalimantacin B (PDB ID 6TBC; Cα r.m.s.d. = 0.150 Å for 239 atoms), (**C**) $NADP^+$/triclosan (PDB ID 4ALI; Cα r.m.s.d. = 0.192 Å for 214 atoms),[18] (**D**) NADPH/CG400549 (PDB ID 4CV1; Cα r.m.s.d. = 0.221 Å for 203 atoms),[21] (**E**) $NADP^+$/compound **8** (PDB ID 4NZ9; Cα r.m.s.d. = 0.226 Å for 210 atoms) and (**F**) 3'-NADPH/AFN-1252 (PDB ID 4FS3; Cα r.m.s.d. = 0.274 Å for 213 atoms).[22] Structures solved herein are colored teal (saFabI), with gold (kalimantacin A), salmon (kalimantacin B) or white (NADPH) carbons; other structures are colored grey (saFabI), with blue (inhibitor) or white (NADP(H) or analog) carbons. Inhibitor structure, name, and class are given at the top of each panel.

The FabI/NADPH/kalimantacin A complex is further stabilized by six specific interactions. The carboxy terminus and adjacent vinyl group of kalimantacin A form π-stacking interactions with the nicotinamide ring of NADPH, further allowing the carboxylic acid group to form hydrogen bonds with

the 2′-OH of the ribose moiety of NADPH (2.6 ± 0.2 Å) and the side chain of Y157 (2.6 ± 0.2 Å) (Figure 1D).[18] These contacts, which appear to be crucial for the recognition of many known FabI inhibitors, mimic the interactions observed with the thioester carbonyl of the acyl-ACP enolate intermediate during the reductase reaction.[20] Indeed, superposition of our structure with that of the *Mycobacterium tuberculosis* FabI ortholog bound to NAD^+ and C_{16}-*N*-acetylcysteamine (PDB ID 1BVR)[23] shows that kalimantacin A utilizes its unique distribution of sp^2- and sp^3-hybridized carbons to closely mimic the bent conformation of the natural fatty acyl substrate (Figure 3). Kalimantacin A also binds to the backbone atoms of A97 which normally interact with the terminal phosphopantetheine amide in the natural substrate: the C-19 carbonyl oxygen atom of kalimantacin A forms a hydrogen bond with the amide hydrogen atom (3.0 ± 0.1 Å) while the C-17 hydroxyl group is hydrogen bonded to the carbonyl oxygen atom (2.7 ± 0.2 Å). Finally, the hydrogen atoms of the carbamate NH_2 in kalimantacin A associate via hydrogen bonds with the oxygen atom of the backbone carbonyl in A95 (2.8 ± 0.2 Å) and the side chain of S197 (2.9 ± 0.1 Å), thereby forming a bridge between the two flexible substrate binding loops SBL-1 and SBL-2 (residues I94-E108). Energy minimization analysis of the crystal structure indicates that the S197 side chain also has the potential to interact with the carboxylate oxygen of kalimantacin (~3.0 Å), further strengthening the hydrogen bonding network between the enzyme, cofactor and antibiotic. Like A97, S197 is predicted to position the phosphopantetheine amide group when the natural enoyl-ACP substrate binds.[20]

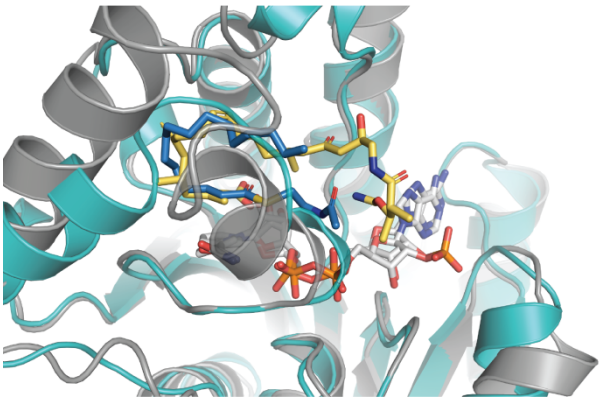

Figure 3. Kalimantacin A binds saFabI with interactions both resembling and differing from those of a substrate analog. Superposition of an saFabI monomer bound to NADPH/KLA with an *M. tuberculosis* InhA (FabI ortholog) monomer bound to NAD^+ and a C_{16}-*N*-acetylcysteamine (C_{16}-*S*-NAC) substrate analog (PDB ID 1BVR); Cα r.m.s.d. of 0.920 Å for 180 atoms). Colour code: saFabI (teal) bound to kalimantacin A (gold carbons) and NADPH (white carbons); InhA (grey) bound to C_{16}-*S*-NAC (blue carbons) and $NADP^+$ (white carbons). While the structures generally align well, major rearrangements in a few secondary structural elements near the active site give a diverging Cα r.m.s.d.

To investigate the effect of kalimantacin A on the catalytic activity of saFabI, a series of *in vitro* enzymatic assays and kinetic studies were performed using crotonoyl-CoA as a mimic of the natural substrate.[18] The ability of FabI to consume NADPH in the presence of varying concentrations of the antibiotic was examined by monitoring the decrease in absorption at 340 nm (Figure 4A). In this assay, saFabI was inhibited by kalimantacin with an IC_{50} of 1.51 μM (Figure 4B). In comparison, we determined the IC_{50} value for triclosan as 5.71 μM.

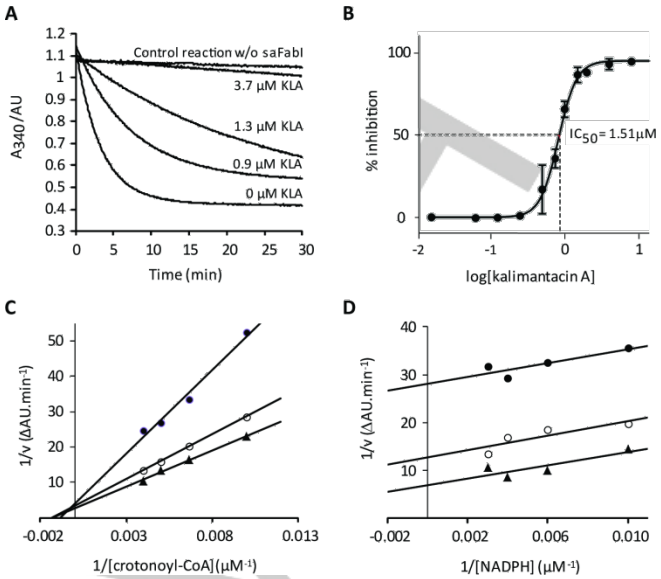

Figure 4. Mechanism of inhibition of saFabI by kalimantacin A. (**A**) Analysis of NADPH consumption in the saFabI-catalyzed reduction of crotonoyl-CoA in the presence of varying concentrations of kalimantacin A. The absorption at 340 nm was monitored continuously for 30 min. (**B**) IC_{50} determination of kalimantacin A. (**C** and **D**) Identification of the mechanism of inhibition of kalimantacin A with respect to (**C**) crotonoyl-CoA and (**D**) NADPH. Initial reaction velocities in the presence of 0 μM (▲), 0.91 μM (○) and 1.37 μM (●) kalimantacin A were plotted against substrate concentrations in double reciprocal plots. The markers represent the mean of three independent replicates. Data were fitted against the Morrison equation to obtain the K_i.

The kinetics of saFabI inhibition were analyzed by measuring the initial rates of NADPH oxidation. Assays were performed by varying the concentration of crotonoyl-CoA at a saturating concentration of NADPH and *vice versa*. The concentration of kalimantacin A in these reactions was varied from 0 to 1.35 μM. The mode of inhibition for kalimantacin A was determined by visualizing the kinetic data in Lineweaver-Burk plots and fitting the data points to the Morrison equation (Figure 3C and 3D). The results show that kalimantacin A is a competitive inhibitor of crotonoyl-CoA with a K_i of 1.45 ± 0.35 μM, and an uncompetitive inhibitor with respect to NADPH (K_i = 0.69 ± 0.13 μM). This inhibition pattern indicates that kalimantacin A binds to the FabI/NADPH complex to prevent substrate binding. This is in contrast with diphenyl ethers, such as triclosan, which bind exclusively to the enzyme/$NADP^+$ complex generated by catalysis.[6]

Despite its promising biological activity, little is known about the structure-activity relationship of kalimantacin A. Kalimantacin B (**2**, Figure 1A) has previously been reported to be produced by *Alcaligenes* sp. YL-02632S as a minor congener of **1** with four- to eight-fold reduced activity against *S. aureus*. To understand the structural basis for its reduced potency, we purified kalimantacin B from a large-scale culture of *P. fluorescens* BCCM_ID9359 for co-crystallization experiments with saFabI and NADPH (Supplementary Table 2 and Supplementary Figures 4-8). A single crystal consisting of all three components diffracted to ~2.55 Å (Supplementary Table 1). Interestingly, in spite of its lower activity, kalimantacin B was observed in the active site of saFabI in a conformation similar to that of kalimantacin A (Figure 1D). In some monomers, minor differences were found in the orientations of S197 and the

carbamate group of the antibiotic, allowing for a hydrogen bond between the Ser side chain and bridging oxygen atom of the carbamate moiety (2.9 ± 0.6 Å). However, this interaction may also be plausible for kalimantacin A given slight bond rotations. Weaker electron density for kalimantacin B relative to its isomer, particularly in the conjugated region, suggests that kalimantacin B experiences greater mobility within its binding cleft (Supplementary Figure 2).

To gain more insight into the binding affinities of kalimantacin A and B, we performed 200 ns molecular dynamics (MD) simulations with our co-crystal structures and calculated binding free energies. During the simulations, the enzyme active site exhibited greater flexibility in the presence of kalimantacin B than its *E,Z*-diene isomer. In the kalimantacin B complex, a slight displacement of the adenosine moiety in the NADPH cofactor was observed, along with a minor displacement of the substrate binding loop SBL-1 (Supplementary Figure 9). Due to the *E,E*-configuration of its diene moiety, kalimantacin B is unable to adopt exactly the same conformation in the active site as kalimantacin A. This slightly reduces its ability to clamp down on the NADPH cofactor. Indeed, while only a slight difference in calculated binding affinity was observed between both isomers, kalimantacin A was found to stabilize NADPH binding (ΔG_{NADPH} = -87.95 ± 5.54 kcal/mol, ΔG_{KLA} = -56.24 ± 2.34 kcal/mol) significantly more than kalimantacin B (ΔG_{NADPH} = -68.02 ± 4.42 kcal/mol, ΔG_{KLB} = -58.16 ± 2.61 kcal/mol).

Two other kalimantacin-related metabolites, 17-hydroxy (**3**) and 27-descarbamoyl (**4**) kalimantacin A, were previously isolated from *P. fluorescens* BCCM_ID9359 mutants with in-frame deletions in the kalimantacin biosynthetic gene cluster (Supplementary Table 3).[10] Their activity against *S. aureus* ATCC 6538 was shown to be reduced 62.5- and 8-fold, respectively, compared to kalimantacin A (Minimal Inhibitory Concentration, MIC = 0.064 μg/ml).[10] These data indicate that the hydrogen bonding interactions with S197, A95 and especially the backbone carbonyl of A97 are essential for the proper positioning of the antibiotic within the FabI active site. To further probe the importance of functional groups for target site recognition, a panel of derivatives was synthesized and evaluated for its ability to inhibit the growth of *S. aureus* ATCC 6538. Replacement of the terminal carboxylic acid group in kalimantacin with a carboxamide moiety (**5**) resulted in reduced potency (MIC = 2 μg/ml), while compounds with various substituents on the 1-OH or -NH_2 group (**6**-**8**) completely lost their anti-staphylococcal activity (Supplementary Table 3). These results confirm the importance of polar interactions between the antibiotic and both the ribose moiety of NADPH and the side chain of Y157. Indeed, the same contacts are utilized by many known FabI inhibitors from various different compound classes.[20] Modification of 19-OH with an acetyl group (**9**) was also not well tolerated (MIC = 2 μg/ml) and the potency of this compound further decreased when the amino group of the carbamate moiety was replaced with a methyl group (**10**) (MIC = 16 μg/ml).

It has previously been shown that *S. aureus* can acquire resistance to kalimantacin A *in vitro*.[24] To investigate the underlying mechanism(s) of resistance development, serial passage experiments were performed by growing *S. aureus* NCTC 8325 on LB agar plates containing increasing concentrations of the antibiotic. Three independently isolated kalimantacin-resistant strains which could grow at 256 times the MIC were selected after eight serial passages. The genomic DNA of the three resistant strains and the parent strain was isolated and sequenced by highly parallel pyrosequencing. A

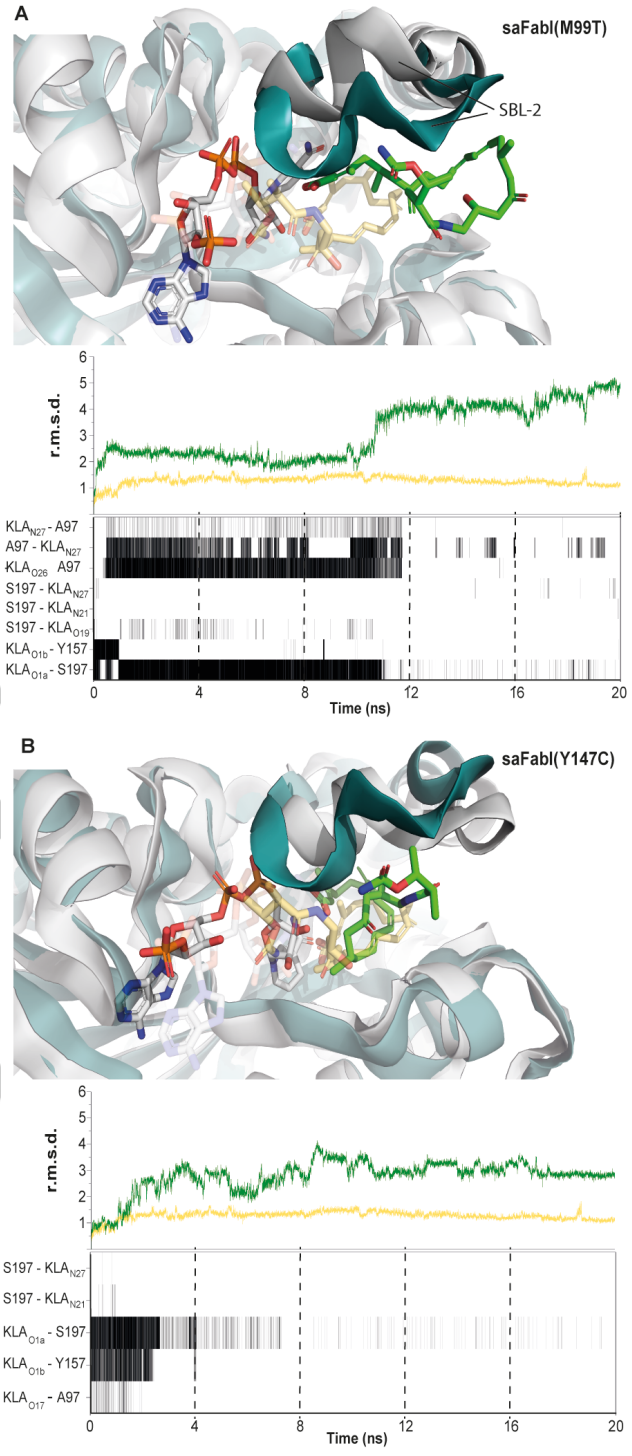

Figure 5. MD simulations of saFabI(M99T) and saFabI(Y147C) in complex with NADPH and kalimantacin A. Superposition of the wild-type saFabI/NADPH/KLA complex and the corresponding **(A)** saFabI(M99T) and (**B**) saFabI(Y147C) complex generated by 20 ns MD simulations. Colour code: wild-type saFabI (teal) bound to KLA (yellow carbons) and NADPH (white faded carbons); mutant saFabI enzymes (grey) bound to KLA (green carbons) and NADPH (white carbons). R.m.s.d. plots in time (20 ns) showing the dynamic motion of the KLA backbone atoms in the wild-type saFabI complex (yellow lines), versus the mutant saFabI complexes (green lines, top and bottom plot, respectively) are shown below the structures. Hydrogen bond decomposition analyses for KLA in both mutant saFabI complexes are shown below each r.m.s.d. plot.

total of six significant single nucleotide polymorphisms (SNPs) were identified (Supplementary Table 4). Two mutations were found in all kalimantacin-resistant mutants. The first mutation (thymine 919,922 to guanine) was located 109 nucleotides upstream of *fabI* in the promoter region (-109 T>G), while the second (adenine 920,470 to guanine) occurred within the *fabI* coding sequence where it caused a Tyr to Cys change at amino acid residue 147 (Y147C). Two other mutations were shared by two of the three resistant strains. One of these (thymine 920,326 to cytosine) was also located in *fabI*, causing a Met to Thr change at amino acid residue 99 (M99T), while the other (adenine 919,959 to guanine) was found 72 nucleotides upstream of *fabI* (-72 A>G). The final two SNPs, which were only found once, were mapped to an intergenic region and a putative pyruvate kinase gene.

The accumulation of point mutations in the *fabI* coding sequence and promoter region is a known resistance mechanism against FabI inhibitors in *S. aureus*. The mutations that occur 109 and 72 bp upstream of *fabI* have previously been identified in triclosan-resistant clinical *S. aureus* isolates and have been linked to increased *fabI* expression.[25] Thymine -109 is located within the DNA recognition sequence of the transcriptional repressor FapR, while adenine -72 lies between the predicted -10 and -35 promoter sequences. Y147 is located in the active site of FabI and is proposed to play an essential role in hydration of the substrate binding pocket.[20] Replacement of this residue with His (Y147H) has been reported to confer resistance to the inhibitors triclosan, AFN-1252 and CG400462.[22,26] A Y147C mutation has not been observed to date. M99, which forms part of the flexible SBL-2 loop adjacent to the FabI active site, has also been found mutated in *S. aureus* isolates with decreased susceptibility to AFN-1252, and the combined presence of Y147H and M99T further increased the MIC of these antibiotics.[27]

To confirm that the *fabI* mutations were responsible for the reduced kalimantacin susceptibility in *S. aureus* and to examine their effect on the activity of saFabI, we introduced the mutations in an *safabI* overexpression vector (pET28a-*fabI*), both separately and in the observed combination. The resulting saFabI variants were overproduced in *E. coli* and purified as described for the wild-type enzyme (Supplementary Figure 10). To investigate their catalytic activity, the consumption of NADPH was monitored in the presence of crotonoyl-CoA (Supplementary Figure 11). The Y147C mutant and the M99T/Y147C double mutant of saFabI showed little or no activity in these reactions, most likely due to protein stability issues. This phenomenon has previously been reported for other FabI mutants.[27] The M99T mutant did show activity *in vitro* and was therefore assayed for its resistance to kalimantacin. However, no reliable IC_{50} value could be obtained.

To circumvent the challenges associated with the stability of the purified recombinant saFabI mutants, we utilized an *in vivo* complementation assay to examine their functionality. The wild-type and mutant *safabI* genes were cloned together with the native *safabI* promoter region into the broad-host-range expression vector pJH10, and the resulting constructs were used to transform the temperature-sensitive (Ts) *fabI* mutant strain *E. coli* JP1111. This strain is unable to grow at the non-permissive temperature of 42 °C unless a functional FabI enzyme is present.[28] As expected, heterologous expression of the wild-type *safabI* gene was able to complement the Ts *fabI* mutation of *E. coli* JP1111 and support its growth at the nonpermissive temperature (Supplementary Figure 12). Likewise, all saFabI mutants displayed *in vivo* enoyl-ACP reductase activity in these experiments.

Table 1. Activity of kalimantacin A against *S. aureus* strains expressing wildtype or mutant *safabI* genes.

Strain	MIC kalimantacin A (μg/ml)
S. aureus ATCC6538	0.064
S. aureus RN4220	0.125
+ pSK5632	0.125
Native *safabI* promoter	
+ pSK5632(*safabI*)	0.125
+ pSK5632(*safabI(M99T)*)	0.5
+ pSK5632(*safabI(Y147C)*)	0.5
+ pSK5632(*safabI(M99T,Y147C)*)	16
***(-109T>G) safabI* promoter**	
+ pSK5632(*safabI*)	0.125
+ pSK5632(*safabI(Y147C)*)	4
***(-72A>G,-109T>G) safabI* promoter**	
+ pSK5632(*safabI*)	0.5

We next examined whether the amino acid changes in saFabI confer resistance to kalimantacin A by determining MIC values against *S. aureus* RN4420 strains expressing the mutant *safabI* genes. For expression in *S. aureus* RN4220, *safabI* and the mutant variants were cloned under the control of the native *fabI* promoter in the low copy number expression vector pSK5632. The MIC of kalimantacin against the parental strain was determined as 0.125 μg/mL, and no change in MIC value was observed when the empty vector was introduced or when the wild-type *safabI* gene was expressed. On the other hand, expression of either saFabI(Y147C) or saFabI(M99T) induced a four-fold increase in the MIC of kalimantacin (MIC = 0.5 μg/ml), and RN4220 cells expressing the M99T/Y147C double mutant were almost completely resistant (MIC = 16 μg/ml) (Table 1). Upon introduction of the observed promoter mutations (-72 A>G and -109 T>G) into the pSK5632-*safabI* expression construct, the MIC of kalimantacin A increased four-fold. The -109 T>G mutation alone did not lead to an increase in resistance. However, when it was introduced into the *safabI(Y147C)* expression vector, an eight-fold increase in the MIC was observed compared to RN4420 cells carrying the construct with the native *safabI* promoter. These results are consistent with previous observations linking -72 A>G and -109 T>G with elevated *safabI* expression and reduced triclosan susceptibility.[25]

As discussed above, both M99 and Y147 appear to contribute to the binding of kalimantacin A via hydrophobic interactions (Figure 1D). To better understand the effect of the mutations on kalimantacin resistance, we performed 20 ns MD simulations based on our structure of the saFabI/NADPH/KLA

ternary complex (Figure 5). Simulations with tetrameric saFabI(M99T) revealed that the binding pose of kalimantacin A is disrupted after approximately 10 ns, causing the antibiotic to lose its interactions with key binding site residues. M99 resides on the flexible substrate binding loop SBL-2 that forms a structured lid over the active site following the binding of NADPH and the substrate or inhibitor. In all saFabI(M99T)/NADPH/KLA simulations, the lid gradually opened by 4.7 Å over the first 8 ns, causing kalimantacin A to drift away from the binding pocket. This observation is supported by r.m.s.d. plots, where an initial deviation of ~2 Å in the binding pose of the antibiotic is observed after 2 ns, followed by a 4.5 Å deviation after 10 ns. These results indicate that M99 plays an important role in stabilizing the closed conformation of SBL-2 during binding of kalimantacin A.

In simulations with saFabI(Y147C), the binding pose of the antibiotic is disrupted more rapidly but less severely (Figure 5). The terminal carboxylic acid group loses its contacts with Y157 and NADPH, while the carbamate moiety loses its hydrogen bonds to A95 and S197. This is also evident from r.m.s.d. plots, where the initial binding pose of kalimantacin A shifts by ~3 Å after 2 ns. The loss of interactions with the antibiotic triggers a major displacement of the adenosine moiety in the cofactor. Compared to the simulations with saFabI(M99T), only a minor opening of the SBL-2 loop (1.3 Å) is observed, and the central hydrophobic portion of the antibiotic largely remains inside the binding pocket. These results underline the importance of Y147 in stabilizing the anchoring interactions with Y157 in saFabI and NADPH that keep the carboxylic acid group of kalimantacin A in position.

In conclusion, we have elucidated the structural and mechanistic basis for the action of the kalimantacin antibiotics, revealing a unique mode of interaction with the essential *S. aureus* enzyme FabI. A recent study has shown that the biosynthetic machinery responsible for the assembly of the kalimantacins exerts precise control over the incorporation of the different β-branching modifications at C-3, C-5, C-7 and C-15 in the antibiotics.[14] It is now clear that the kalimantacins utilize this specific pattern of sp^2- and sp^3-hybridized carbons to mimic the bent conformation of the natural enoyl-ACP substrate. Our findings thus offer inspiration for the design and development of a new generation of saFabI inhibitors that can be used to combat the escalating public health crisis caused by multidrug-resistant *S. aureus* infections.

Acknowledgements

This research was supported by grants from the European Commission (through a Marie Sklodowska-Curie Fellowship to JM; contract no. 656067) and the Research Foundation Flanders (to JM). Network on Antimicrobial Resistance in Staphylococcus aureus (NARSA) Chantilly, Virginia 20151 USA is acknowledged for providing the *Staphylococcus aureus* NCTC 8325 strain.

Keywords: antibiotics • inhibitors • natural products • methicillin-resistant *Staphylococcus aureus* (MRSA) • protein structures

[1] a) G. L. Archer, *Clin. Infect. Dis.* **1998**, *26*, 1179–81; b) N. F. Al-Mebairik, T. A. El-Kersh, Y. A. Al-Sheikh, M. A. M. Marie, *Rev. Med. Microbiol.* **2016**, *27*, 50–56.

[2] a) World Health Organization, *The Evolving Threat of Antimicrobial Resistance - Options for Action*, **2012**; b) T. J. Foster, *FEMS Microbiol. Rev.* **2017**, *41*, 430–449.

[3] R. J. Heath, C. O. Rock, *Curr. Opin. Investig. Drugs* **2004**, *5*, 146–153.

[4] W. Balemans, N. Lounis, R. Gilissen, J. Guillemont, K. Simmen, K. Andries, A. Koul, *Nature* **2010**, *463*, E3.

[5] F. J. Asturias, J. Z. Chadick, I. K. Cheung, H. Stark, A. Witkowski, A. K. Joshi, S. Smith, *Nat. Struct. Mol. Biol.* **2005**, *12*, 225–232.

[6] H. Xu, T. J. Sullivan, J. Sekiguchi, T. Kirikae, I. Ojima, C. F. Stratton, W. Mao, F. L. Rock, M. R. K. Alley, F. Johnson, et al., *Biochemistry* **2008**, *47*, 4228–4236.

[7] H. Bergler, S. Fuchsbichler, G. Högenauer, F. Turnowsky, *Eur. J. Biochem.* **1996**, *242*, 689–694.

[8] a) R. J. Heath, N. Su, C. K. Murphy, C. O. Rock, *J. Biol. Chem.* **2000**, *275*, 40128–40133; b) R. P. Massengo-Tiassé, J. E. Cronan, *J. Biol. Chem.* **2008**, *283*, 1308–1316; c) H. Marrakchi, W. E. Dewolf, C. Quinn, J. West, B. J. Polizzi, C. Y. So, D. J. Holmes, S. L. Reed, R. J. Heath, D. J. Payne, et al., *Biochem. J.* **2003**, *370*, 1055–1062.

[9] a) R. J. Heath, C. O. Rock, *Nature* **2000**, *406*, 145–146; b) L. Zhu, J. Lin, J. Ma, J. E. Cronan, H. Wang, *Antimicrob. Agents Chemother.* **2010**, *54*, 689–698.

[10] W. Mattheus, L. J. Gao, P. Herdewijn, B. Landuyt, J. Verhaegen, J. Masschelein, G. Volckaert, R. Lavigne, *Chem. Biol.* **2010**, *17*, 149–159.

[11] V. V Smirnov, L. N. Churkina, A. N. Kravets, A. D. Garagulia, *Antibiot. i khimioterapiia* **1993**, *38*, 3–5.

[12] K. Kamigiri, Y. Suzuki, M. Shibazaki, M. Morioka, K.-I. Suzuki, T. Tokunaga, B. Setiawan, R. M. Rantiamodjo, *J. Antibiot. (Tokyo).* **1996**, *49*, 136–139.

[13] I. R. G. Thistlethwaite, F. M. Bull, C. Cui, P. D. Walker, S.-S. Gao, L. Wang, Z. Song, J. Masschelein, R. Lavigne, M. P. Crump, et al., *Chem. Sci.* **2017**, *8*, 6196–6201.

[14] P. D. Walker, C. Williams, A. N. M. Weir, L. Wang, J. Crosby, P. R. Race, T. J. Simpson, C. L. Willis, M. P. Crump, *Angew. Chemie Int. Ed.* **2019**, *58*, 12446–12450.

[15] L. Churkina, E. Kiprianova, S. Bidnenko, K. Marchenko, E. Artysyuk, *Likars'ka Sprav.* **2009**, *1–2*, 61–67.

[16] L. Churkina, M. Vaneechoutte, E. Kiprianova, N. Perunova, L. Avdeeva, O. Bukharin, *Open J. Med. Microbiol.* **2015**, *5*, 193–201.

[17] a) V. E. Lee, A. J. O'Neill, *Int. J. Antimicrob. Agents* **2017**, *49*, 121–122; b) W. Mattheus, J. Masschelein, L. J. Gao, P. Herdewijn, B. Landuyt, G. Volckaert, R. Lavigne, *Chem. Biol.* **2010**, *17*, 1067–1071.

[18] J. Schiebel, A. Chang, H. Lu, M. V Baxter, P. J. Tonge, C. Kisker, *Structure* **2012**, *20*, 802–813.

[19] E. Krissinel, K. Henrick, *J. Mol. Biol.* **2007**, *372*, 774–797.

[20] J. Schiebel, A. Chang, B. Merget, G. R. Bommineni, W. Yu, L. A. Spagnuolo, M. V Baxter, M. Tareilus, P. J. Tonge, C. Kisker, et al., *Biochemistry* **2015**, *54*, 1943–1955.

[21] J. Schiebel, A. Chang, S. Shah, Y. Lu, L. Liu, P. Pan, M. W. Hirschbeck, M. Tareilus, S. Eltschkner, W. Yu, et al., *J. Biol. Chem.* **2014**, *289*, 15987–16005.

[22] N. Kaplan, M. Albert, D. Awrey, E. Bardouniotis, J. Berman, T. Clarke, M. Dorsey, B. Hafkin, J. Ramnauth, V. Romanov, et al., *Antimicrob. Agents Chemother.* **2012**, *56*, 5865–5874.

[23] D. A. Rozwarski, C. Vilchèze, M. Sugantino, R. Bittman, J. C. Sacchettini, *J. Biol. Chem.* **1999**, *274*, 15582–15589.

[24] L. Churkina, Z. Vasyurenko, S. Bidnenko, M. Vaneechoutte, *Likars'ka Sprav.* **2007**, *3*, 50–56.

[25] D. Grandgirard, L. Furi, M. L. Ciusa, L. Baldassarri, D. R. Knight, I. Morrissey, C. R. Largiadèr, S. L. Leib, M. R. Oggioni, *BMC Genomics* **2015**, *16*, 345.

[26] a) H. S. Park, Y. M. Yoon, S. J. Jung, I. N. R. Yun, C. M. Kim, J. M. Kim, J.-H. Kwak, *Int. J. Antimicrob. Agents* **2007**, *30*, 446–451; b) N. P. Brenwald, A. P. Fraise, *J. Hosp. Infect.* **2003**, *55*, 141–144.

[27] J. Yao, J. B. Maxwell, C. O. Rock, *J. Biol. Chem.* **2013**, *288*, 36261–36271.

[28] a) H. Bergler, G. Hogenauer, F. Turnowsky, *J. Gen. Microbiol.* **1992**, *138*, 2093–2100; b) H. Bergler, S. Fuchsbichler, G. Hogenauer, F. Turnowsky, *Eur. J. Biochem.* **1996**, *242*, 689–694; c) A. F. Egan, R. R. Russell, *Genet. Res.* **1973**, *21*, 139–52.

COMMUNICATION

The kalimantacin antibiotics mimic the conformation of the natural fatty acyl substrate to inhibit the activity of the essential enoyl-ACP reductase enzyme FabI in *Staphylococcus aureus*

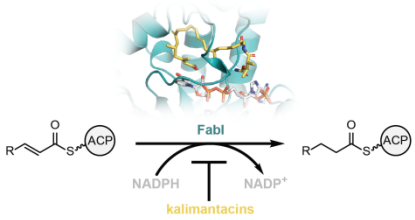

*Christopher D Fage†, Thomas Lathouwers†, Michiel Vanmeert, Ling-Jie Gao, Kristof Vrancken, Eveline-Marie Lammens, Angus NM Weir, Ruben Degroote, Harry Cuppens, Simone Kosol, Thomas J Simpson, Matthew P Crump, Christine L Willis, Piet Herdewijn, Eveline Lescrinier, Rob Lavigne, Jozef Anné and Joleen Masschelein**

Page No. – Page No.

The kalimantacin polyketide